Hindawi
Advances in Mathematical Physics
Volume 2020, Article ID 5631684, 6 pages
https://doi.org/10.1155/2020/5631684

Research Article

Joining between Boron Nitride Nanocones and Nanotubes

Nawa Alshammari

Department of Mathematics, College of Science and Theoretical Studies, Saudi Electronic University, Saudi Arabia

Correspondence should be addressed to Nawa Alshammari; n.alshammari@seu.edu.sa

Received 25 March 2020; Accepted 16 April 2020; Published 30 April 2020

Academic Editor: Marin Marin

Different nanostructures of boron nitride have been observed experimentally such as fullerenes, tubes, cones, and graphene. They have received much attention due to their physical, chemical, and electronic properties that lead them to numerous applications in many nanoscale devices. Joining between nanostructures gives rise to new structures with outstanding properties and potential applications for the design of probes for scanning tunneling microscopy and other nanoscale devices, as carriers for drug delivery and liquid separation. This paper utilizes calculus of variations to model the joining between two types of BN nanostructures, namely, BN nanotubes and BN nanocones. Based on the curvature of the join curve, the joining of these structures can be divided into two models. Model I refers to when the join profile includes positive curvature only, and Model II contains both positive and negative curvatures. The main goal here is to formulate the basic underlying structure from which any such small perturbations can be viewed as departures from an ideal model. For this scenario of joining, we successfully present simple models based on joining BN nanotubes to BN nanocones with five different angles of the cone.

1. Introduction

Boron nitride (BN) nanostructures have been the focus of extensive research area in current years. BN nanostructures are chemical compounds containing atoms of boron and nitrogen. They are similar to carbon nanomaterials in their geometrical structures and vary in their physiochemical properties. In particular, BN in nanoscale materials are important because of their electronic, optical, mechanical, and magnetic properties. Moreover, they have high oxidation resistance, high thermal conductivity, constant wide band gap, and lower toxicity. This makes them a promising candidate for application in different conditions [1]. Similar to carbon nanostructures, BN in nanoscale has different structures such as nanotubes, sheets, fullerenes, and nanocones [2].

Boron nitride nanotubes (BNNTs) were first predicated in 1994 and synthesized in 1995. BNNTs can be created by rolling graphene sheet as a cylinder. They have significant attention in recent years due to their different physical properties. For example, they have high thermal conductivity, mechanical strength with an elastic modulus of 1.2 TPa, and wide band gap of about 5.5 eV with exceptional radiation shielding compared to carbon NTs [3, 4]. In addition, they are stable in air and in an inert atmosphere. Based on these fantastic properties, BNNTs have different applications such as in biomedical applications specially in drug delivery and bone scaffolding, electronic and microelectronic mechanical devices, and energy storage [3, 5, 6]. Also, they can be used as alternative to CNTs to help enhance strength of materials [4].

BN nanocones are another form of BN nanostructures. BNNCs are discovered in 1994 as cap nanotubes end; then, they are synthesized as free structures by different groups. BNNCs can be made by rolling nanostructure sheet [1, 7]. Their physical, chemical, and electronic features such as chemical oxidation inertness, mechanical toughness, and thermal stability attract researchers' more attention to explore their potential applications in different aspects [2, 8].

Joining nanostructures can enhance the physiochemical and trochemical performance of the joined structures with new applications. In particular, the new produced structures are useful for the design of probes for scanning tunneling microscopy, energy storage, and other electronic devices as carriers for drug delivery [9].

Researches in [9], [10–13] minimize the elastic energy which depends on the axial curvature only by using calculus

of variations to determine the joining curve between two carbon nanostructures. Following [9–14], this paper extends this model to determine the joining curve between two boron nitride nanostructures: BN nanotubes and BN nanocones. We comment that this model does not take into account the chemical issues, such as positions of atoms and bonds. Finally, using Willmore energy which depends on the axial and rotational curvatures to determine the joining between nanostructures gives rise to similar joining profiles of using elastic energy as studied in [15]. Furthermore, similar techniques have been used and investigated by many researches such as in [16–18] and [19].

In the following section, we state the fundamental equations of the calculus of variations to model the joining region between BNNTs and BNNCs. Namely, Model I denotes positive joining curvature while Model II denotes positive and negative joining curvatures. Results and discussion are given in Section 3. Section 4 provides the conclusion.

2. Model

In this section, the basic variational equations of the model that is used to join boron nitride nanocone and boron nitride nanotube are formulated. In particular, variational calculus is used to specify the curve adopted by a line smoothly connecting BN nanocone base to a vertical BN nanotube, where the arc length of the joining curve and the defect site at the BN nanocone base are specified. Thus, the distance in y-direction y_0 of the join to the cylindrical tube is not specified and it is found as a part of the solution.

Using calculus of variations to find the curve $y(x)$, with an element of arc length ds, which minimizes the energy functional $J[y]$ that is given by

$$J[y] = \int_0^{\ell} \kappa^2 ds + \lambda \int_0^{\ell} ds, \tag{1}$$

where κ is the curvature, λ is a Lagrange multiplier corresponding to the fixed length constraint, and ℓ is the length of the joining curve. The boundaries of the join region are x_0 and x_1, where at $x = x_0$; we have $s = 0$, and at $x = x_1$; we have $s = \ell$. For a curve in two dimensions described as a graph $y = y(x)$, we have $\kappa = \ddot{y}/(1+\dot{y}^2)^{3/2}$, and $ds = (1+\dot{y}^2)^{1/2} dx$, so that equation (1) becomes

$$J[y] = \int_a^{b \sin(\gamma/2)} \frac{\ddot{y}^2}{(1+\dot{y}^2)^{5/2}} dx + \lambda \int_a^{b \sin(\gamma/2)} (1+\dot{y}^2)^{1/2} dx, \tag{2}$$

where throughout this paper, dot denotes differentiation with respect to x. Applying the delta variational operator and integration by parts twice, the standard equation can be written as

$$\begin{aligned} \delta J[y] = &\left[\left(F_{\dot{y}} - \frac{d}{dx} F_{\ddot{y}} \right) \delta y + F_{\ddot{y}} \delta \dot{y} \right]_a^{b \sin(\gamma/2)} \\ &+ \int_a^{b \sin(\gamma/2)} \left(F_y - \frac{d}{dx} F_{\dot{y}} + \frac{d^2}{dx^2} F_{\ddot{y}} \right) \delta y dx, \end{aligned} \tag{3}$$

where subscripts denote partial derivatives and here the function F is given by

$$F(\dot{y}, \ddot{y}) = \frac{\ddot{y}^2}{(1+\dot{y}^2)^{5/2}} + \lambda (1+\dot{y}^2)^{1/2}. \tag{4}$$

By imposing the continuity of the function y and its derivatives, the boundary conditions at the join to the nanocone can be determined as

$$\begin{aligned} y\left(b \sin\left(\frac{\gamma}{2}\right)\right) &= b \cos\left(\frac{\gamma}{2}\right), \\ \dot{y}\left(b \sin\left(\frac{\gamma}{2}\right)\right) &= \cot \frac{\gamma}{2}. \end{aligned} \tag{5}$$

As the height of the nanotube y_0 is unknown, we require the natural or alternative boundary condition given by

$$\left[\left(F_{\dot{y}} - \frac{d}{dx} F_{\ddot{y}} \right) \right]_{x=a} = 0. \tag{6}$$

The value of $\dot{y}$, in Model I, ranges from $\cot(\gamma/2)$, at $x = b \sin(\gamma/2)$, to ∞ at $x = a$. Thus, the boundary condition for this model is $\dot{y}(a) = \infty$. For Model II, $\dot{y}$ ranges from $\cot(\gamma/2)$ to ∞, where it changes sign and then ranges from $-\infty$ down to some finite negative value before turning to $-\infty$. Thus, the boundary condition in the case of Model II is $\dot{y}(a) = -\infty$. From equation (3) the usual Euler-Lagrange equation for $F(x, y, \dot{y}, \ddot{y})$, is given by

$$F_y - \frac{d}{dx} F_{\dot{y}} + \frac{d^2}{dx^2} F_{\ddot{y}} = 0. \tag{7}$$

Solving this equation and using the above alternative boundary condition,

$$F - \ddot{y} F_{\ddot{y}} = -\alpha, \tag{8}$$

where α is an arbitrary constant of integration. Now, substituting (4) into (8), the curvature κ can be written as in [11],

$$\kappa = \pm \left(\lambda + \frac{\alpha}{(1+\dot{y}^2)^{1/2}} \right)^{1/2}. \tag{9}$$

2.1. Model I: Positive Curvature. The curvature in Model I is positive along the entire arc length ℓ as shown in Figure 1(a). Based on that, the positive case from (9) is considered only. By using $\dot{y} = \tan\theta$, equation (9) becomes

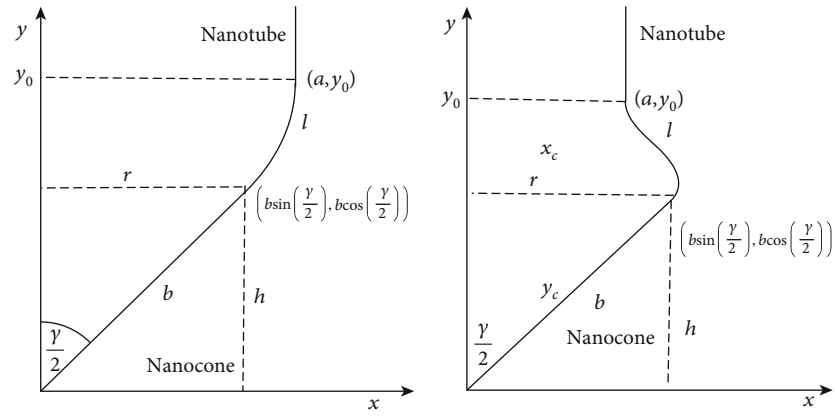

(a) Model I (b) Model II

Figure 1: Model I: positive curvature and Model II: positive and negative curvatures [11].

$$\kappa = (\lambda + \alpha \cos\theta)^{1/2}. \tag{10}$$

From the definition of the curvature $\kappa = \ddot{y}/(1+\dot{y}^2)^{3/2}$, making the same substitution for $\dot{y}$, and simplifying that by introducing a new parametric variable ϕ which is defined by

$$\cos\theta = 1 - 2k^2 \sin^2\phi, \tag{11}$$

where $k = [(\gamma+\alpha)/2\alpha]^{1/2}$, that gives

$$\frac{dy}{d\phi} = 2\beta k \sin\phi, \tag{12}$$

where $\beta = (2/\alpha)^{1/2}$. Now by integrating this equation and using the boundary conditions at the point $(b\sin(\gamma/2), b\cos(\gamma/2))$ of attachment to the nanocone to find the constant of the integration, we have

$$y(\phi) = 2\beta k(\cos\phi_0 - \cos\phi) + b\cos\frac{\gamma}{2}, \tag{13}$$

where

$$\phi_0 = \sin^{-1}\left(\left\{\frac{[1-\sin(\gamma/2)]}{2k^2}\right\}^{1/2}\right), \tag{14}$$

corresponds to $\theta = \pi/2 - \gamma/2$, at the point $(b\sin(\gamma/2), b\cos(\gamma/2))$. Now if we use the boundary condition of the tube open end at the point (a, y_0) with $\phi_t = \sin^{-1}(1/\sqrt{2}k)$, where $\theta = \pi/2$, we find

$$y_0 = 2\beta k(\cos\phi_0 - \cos\phi) + b\cos\frac{\gamma}{2}, \tag{15}$$

and in this model $\theta \in [\pi/2 - \gamma/2, \pi/2]$. Similarly, we derive

$$\begin{aligned} x(\phi) = b\sin\frac{\gamma}{2} + \beta\{&2[E(\phi,k) - E(\phi_0,k)] \\ &- [F(\phi,k) - F(\phi_0,k)]\}, \end{aligned} \tag{16}$$

where $F(\phi,k)$ and $E(\phi,k)$ denote the usual Legendre incomplete elliptic integrals of the first and second kinds, respectively. Using the boundary condition at the point (a, y_0) on the open tube end, we have

$$a- = \beta\{2[E(\phi_t,k) - E(\phi_0,k)] - [F(\phi_t,k) - F(\phi_0,k)]\}. \tag{17}$$

From the definition of the arc length, we have

$$\ell = \int_{b\sin(\gamma/2)}^{a} \left(1+\dot{y}^2\right)^{1/2} dx. \tag{18}$$

Upon substituting $\dot{y} = \tan\theta$, changing the parameter to ϕ as in $\cos\theta = 1 - 2k^2\sin^2\phi$, and integrating, we have

$$\ell = \beta[F(\phi_t,k) - F(\phi_0,k)]. \tag{19}$$

Now, substitute equation (19) into equation (17), we derive

$$\mu = 2\left(\frac{E(\phi_t,k) - E(\phi_0,k)}{F(\phi_t,k) - F(\phi_0,k)}\right) - 1, \tag{20}$$

where $\mu = (a - b\sin(\gamma/2))/\ell$, and $-1 < \mu < 1$. For prescribed values of a, b, γ, and ℓ, equation (20) can be solved numerically to determine the value of k. Then, substituting k into equation (19), the value of β can be determined, and therefore, y_0 can be obtained from (15) [11].

2.2. Model II: Positive and Negative Curvatures. Two regions are considered in this model as shown in Figure 1(b); the first one involves positive curvature from the point of attachment at the nanocone $(b\sin(\gamma/2), b\cos(\gamma/2))$ up until the critical point (x_c, y_c) where the sign of the curvature changed. In this

case, we follow the same process as in the last section. The second region starts from the critical point (x_c, y_c) to the point of attachment at the nanotube (a, y_0) where the curvature is negative. The parameter value of θ as defined in the previous section at the critical point is denoted by θ_c, and from geometrical considerations, we have $0 < \theta_c < \pi/2$. The same process is used to the region of positive curvature where this region is bounded by the point of the curvature $\kappa = 0$; using equation (10), we find

$$\theta_c = \cos^{-1}\left(-\frac{\lambda}{\alpha}\right). \tag{21}$$

Applying the parameter variable ϕ as defined by equation (11), we obtain $\phi = \pi/2$, when $\theta = \theta_c$, and from equation (13) and equation (16), we have the parametric equations for y_c and x_c as

$$y_c = 2\beta k \cos\phi_0 + b\cos\frac{\gamma}{2}, \tag{22}$$

$$x_c = b\sin\frac{\gamma}{2} + \beta\{2[E(k) - E(\phi_0, k)] - [K(k) - F(\phi_0, k)]\}, \tag{23}$$

where β, k, and ϕ_0 are defined in the last section. $F(\phi_0, k)$ and $E(\phi_0, k)$ are defined as the usual incomplete elliptic integrals of the first and second kinds, respectively, and $k(k)$ and $E(k)$ are complete elliptic integrals of the first and second kinds, respectively.

Similarly for the second region, considering the negative sign of equation (9) and integrating, we obtain

$$y(\phi) = 2\beta k(\cos\phi_0 + \cos\phi) + b\cos\frac{\gamma}{2}, \tag{24}$$

noting that when $\phi = \pi/2$, the constant of integration arises from $y = y_c$, and then we use equation (22) for y_c. From the boundary condition at the point of attachment to the nanotube, we have $\phi = \phi_t$, at the point (a, y_0), so we have

$$y_0 = 2\beta k(\cos\phi_0 + \cos\phi_t) + b\cos\frac{\gamma}{2}. \tag{25}$$

Similarly, we take the negative sign of equation (9) and solving for the parametric form of x, we find

$$x(\phi) = b\sin\frac{\gamma}{2} + \beta\{2[2E(k) - E(\phi, k) - E(\phi_0, k)] - [2K(k) - F(\phi, k) - F(\phi_0, k)]\}. \tag{26}$$

At the point (a, y_0) where $\phi = \phi_t$, we have

$$a - b\sin\frac{\gamma}{2} = \beta\{2[2E(k) - E(\phi_t, k) - E(\phi_0, k)] - [2K(k) - F(\phi_t, k) - F(\phi_0, k)]\}. \tag{27}$$

From the two regions, we obtain the arc length constraint as

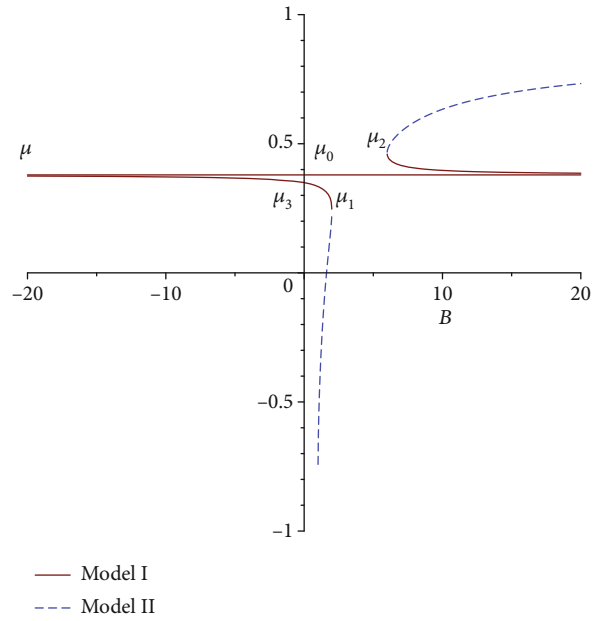

Figure 2: Relation between the parameters $\mu = (a - b\sin(\gamma/2))/\ell$, and $B = 1/k^2$.

$$\ell = \int_{b\sin\gamma/2}^{x_c} \left(1 + \dot{y}^2\right)^{1/2} dx + \int_{x_c}^{a} \left(1 + \dot{y}^2\right)^{1/2} dx, \tag{28}$$

by using $\dot{y} = \tan\theta$, and changing to the parameter ϕ,

$$\ell = \beta[2K(k) - F(\phi_t, k) - F(\phi_0, k)], \tag{29}$$

$$\mu = 2\left(\frac{2E(k) - E(\phi_t, k) - E(\phi_0, k)}{2K(k) - F(\phi_t, k) - F(\phi_0, k)}\right) - 1. \tag{30}$$

We can solve equation (30) numerically to find the value of k, and by substituting k into equation (29), we can determine the value of β so that y_0 can be determined. Noting that equation (20) coincides with (30) for the value $k = 1/\sqrt{2}$, and $k = \{[1 - \sin(\gamma/2)]/2\}^{\sqrt{1/2}}$. For $k = 1/\sqrt{2}$, the value of μ is denoted by μ_1, and when $k = 1/\sqrt{2}$, and $k = \{[1 - \sin(\gamma/2)]/2\}^{\sqrt{1/2}}$, the value of μ is denoted by μ_2 [11].

3. Numerical Results

In this section, we investigate the numerical solution for Model I and Model II when they are characterized by the nondimensional parameter $\mu = [a - b\sin(\gamma/2)]/\ell$. Figure 2 shows the relation between $\mu = [a - b\sin(\gamma/2)]/\ell$, where $-1 < \mu < 1$, and $B = 1/k^2$. There are two main regions; the first region is determined when $\mu < \mu_0$, and the value of $B < 2$, where μ_0 is the asymptotic value for μ when k tends to be zero, given by [11]

$$\mu_0 = 1 + \frac{\sqrt{2}\left(1 - \sqrt{2}\cos\omega\right)}{\ln\left[\left(\sqrt{2} - 1\right)/(\tan(\omega/2))\right]}, \tag{31}$$

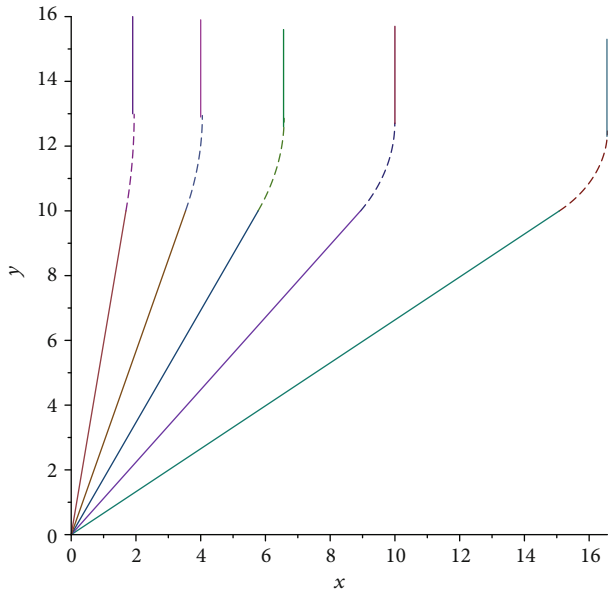

FIGURE 3: Plot of the join $y = y(x)$, for Model I for nanocones with apex angles of 180°, 112.9°, 83.6°, 60°, 38.9°, and 19.2°, $\ell = 3$, and $B = -10$.

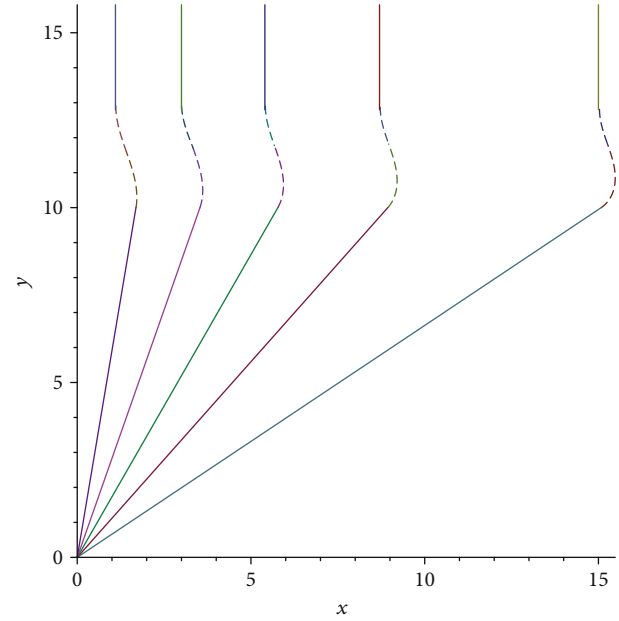

FIGURE 4: Plot of the join $y = y(x)$, for Model II for nanocones with apex angles of 180°, 112.9°, 83.6°, 60°, 38.9°, and 19.2°, $\ell = 3$, and $B = 1.5$.

where $\omega = (\pi - \gamma)/4$. This region may be divided into three subregions. The first subregion is when $\mu_3 < \mu < \mu_0$, where μ_3 is the asymptotic value of μ when k tends to be ∞ [11]

$$\mu_3 = \frac{2}{\gamma}\left(1 - \cos\left(\frac{\gamma}{2}\right)\right). \tag{32}$$

The value of the parameter B in this subregion is negative with a negative value of α an imaginary modulus k for the elliptic functions. The second subregion is $\mu_1 < \mu < \mu_3$, where the value of the parameter B corresponds to $0 < B \leq 2$, with a positive value of α and real k. The third subregion is $-1 < \mu < \mu_1$, where the value of the parameter B is between $1 < B \leq 2$, and positive value for α.

The second region is when $\mu > \mu_0$, where the value of $B > 2/[1 - \sin(\gamma/2)]$. This region also involves two subregions; the first subregion is $\mu_0 < \mu < \mu_2$, which corresponds to Model I, and the second subregion is $\mu_2 < \mu < 1$, which corresponds to Model II. The values of the parameter B for these two subregions are positive with a negative value of α.

Based on the above results, we join nanocones to nanotubes for Model I and Model II as in Figures 3 and 4, respectively. In particular, here, we assume that heights of the cone are equal and the cone radii are found from $r = h \tan(\gamma/2)$. The five possible nanocones have fixed arc length which assumed to be $\ell = 3$.

4. Conclusion

This paper uses conventional applied mathematical modelling in an essentially discrete problem of determining the profiles of the joins between boron nitride nanotubes and boron nitride nanocones. These new combined nanostructures may be useful for the design of probes for scanning tunneling microscopy and other nanoscale devices. In particular, calculus of variations is used to minimize the elastic energy for the joining curve which leads to minimize the covalent bond energy. During this joining, two models are considered depending on the sign of the curvature: Model I refers to the positive curvature only, and Model II refers to both positive and negative curvatures. By considering these two models, we join two boron nitride nanostructures which are nanotubes and nanocones. Because of the real physical composite structures which have undulations included from pentagons in the cone, this system is assumed to be axially symmetric and that is the problem that may be reduced to two dimensions. The main purpose here is to formulate the axially symmetric model to have a reference basis for the comparison of real physical structures where it is believed that the undulations are small. As a result, these models lead to significative approximations to complex structures.

Data Availability

Any data and information used to support the findings of this study will be provided by the author upon request.

Conflicts of Interest

The author declares that there are no conflicts of interests regarding the publication of this paper.

References

[1] E. Vessally, R. Moladoust, S. M. Mousavi-Khoshdel, M. D. Esrafili, A. Hosseinian, and L. Edjlali, "The clcn adsorption on the pristine and al-doped boron nitride nanosheet, nanocage, and nanocone: density functional studies," *Thin Solid Films*, vol. 645, pp. 363–369, 2018.

[2] J. W. Yan and K. M. Liew, "Predicting elastic properties of single-walled boron nitride nanotubes and nanocones using an atomistic-continuum approach," *Composite Structures*, vol. 125, pp. 489–498, 2015.

[3] A. B. Kakarla, C. Kong, W. Kong, and I. Kong, "Synthesis and characterization of boron nitride nanotubes-polycaprolactone nanocomposite," *Materials Science Forum*, vol. 951, no. 4, pp. 39–44, 2019.

[4] L. Takahashi, T. Nakagawa, and K. Takahashi, "Electronic structure of octagonal boron nitride nanotubes," *International Journal of Quantum Chemistry*, vol. 118, no. 11, p. e25542, 2017.

[5] V. Kumar, D. Lahiri, and I. Lahiri, "Synthesis of boron nitride nanotubes and boron nitride nanoflakes with potential application in bioimaging," *Materials Today: Proceedings*, vol. 5, no. 8, pp. 16756–16762, 2018.

[6] G. Fan, S. Zhu, and H. Xu, "Density-functional theory study of the interaction mechanism and optical properties of flavonols on the boron nitride nanotubes," *International Journal of Quantum Chemistry*, vol. 118, no. 7, p. e25514, 2018.

[7] A. Hosseinian, M. Salary, S. Arshadi, E. Vessally, and L. Edjlali, "The interaction of phosgene gas with different bn nanocones: Dft studies," *Solid State Communications*, vol. 269, pp. 23–27, 2018.

[8] E. Brito, T. S. Silva, T. Guerra et al., "Structural and electronic properties of double-walled boron nitride nanocones," *Physica E: Low-dimensional Systems and Nanostructures*, vol. 95, pp. 125–131, 2018.

[9] N. A. Alshammari, N. Thamwattana, J. McCoy, B. Duangkamon, B. Cox, and J. M. Hill, "Modelling joining of various carbon nanostructures using calculus of variations," *Dynamics of Continuous, Discrete and Impulsive Systems Series B: Applications and Algorithms*, vol. 25, pp. 307–339, 2018.

[10] B. J. Cox and J. M. Hill, "A variational approach to the perpendicular joining of nanotubes to plane sheets," *Journal of Physics A: Mathematical and Theoretical*, vol. 41, no. 12, pp. 125203–125212, 2008.

[11] D. Baowan, B. J. Cox, and J. M. Hill, "Modelling the joining of nanocones and nanotubes," *Journal of Mathematical Chemistry*, vol. 49, no. 2, pp. 475–488, 2011.

[12] D. Baowan, B. J. Cox, and J. M. Hill, "A continuous model for the joining of two fullerenes," *Philosophical Magazine*, vol. 88, no. 23, pp. 2953–2964, 2008.

[13] D. Baowan, B. J. Cox, and J. M. Hill, "Modeling the join curve between two co-axial carbon nanotubes," *Zeitschrift fu¨r angewandte Mathematik und Physik*, vol. 63, no. 2, pp. 331–338, 2012.

[14] D. Baowan, B. J. Cox, and J. M. Hill, "Junctions between a boron nitride nanotube and a boron nitride sheet," *Nanotechnology*, vol. 19, no. 7, p. 075704, 2008.

[15] P. Sripaturad, N. A. Alshammari, N. Thamwattana, J. A. McCoy, and D. Baowan, "Willmore energy for joining of carbon nanostructures," *Philosophical Magazine*, vol. 98, no. 16, pp. 1511–1524, 2018.

[16] L. Zhang, M. B. Arain, M. M. Bhatti, A. Zeeshan, and H. Hal-Sulami, "Effects of magnetic Reynolds number on swimming of gyrotactic microorganisms between rotating circular plates filled with nanofluids," *Applied Mathematics and Mechanics*, vol. 41, no. 4, pp. 637–654, 2020.

[17] M. Marin and S. Nicaise, "Existence and stability results for thermoelastic dipolar bodies with double porosity," *Continuum Mechanics and Thermodynamics*, vol. 28, no. 6, pp. 1645–1657, 2016.

[18] M. Marin, R. Ellahi, and A. Chirila, "On solutions of Saint-Venant's problem for elastic dipolar bodies with voids," *Carpathian Journal of Mathesmatics*, vol. 33, pp. 219–232, 2017.

[19] L. Barbu and A. E. Nicolescu, "An overdetermined problem for a class of anisotropic equations in a cylindrical domain," *Mathematical Methods in the Applied Sciences*, pp. 1–9, 2020.